Water Resour Manage (2013) 27:1661–1674
DOI 10.1007/s11269-012-0120-3

Regional Drought Modes in Iran Using the SPI: The Effect of Time Scale and Spatial Resolution

Tayeb Raziei · Isabella Bordi · Luis Santos Pereira

Received: 19 December 2011 / Accepted: 31 July 2012 /
Published online: 11 August 2012

Abstract In the present paper, regional drought modes in Iran are identified applying the Principal Component Analysis (PCA) and Varimax rotation to the Standardized Precipitation Index (SPI) computed on different time scales. Data used include gridded monthly precipitation covering the period 1951–2007 retrieved from the Global Precipitation Climatology Centre (GPCC) archive with different spatial resolutions (2.5, 1 and 0.5° resolution). The objective of the study is twofold: (i) Investigate the stability of drought spatial modes as a function of the SPI time scales used for monitoring the different kinds of drought, (ii) Evaluate the impact of the spatial resolution of gridded data on drought regionalization. For the coarse spatial resolution of 2.5°, results show four drought modes of distinct variability, which remain quite stable when the SPI time scale is varied from 1- to 24-month. Differently, for higher spatial resolutions drought modes appear more sensitive to the index time scale and become less spatially homogeneous as the time scale is increased. Moreover, the number of identified modes (sub-regions) may reduce to three or two, but in all cases the most well defined sub-region appears to be the southern one. This suggests that both the spatial resolution of precipitation data and the time scale may affect drought regionalization, i.e. the number of drought modes and their spatial homogeneity.

Keywords Drought regionalization · SPI · Iran · GPCC gridded data

T. Raziei
Soil Conservation and Watershed Management Research Institute (SCWMRI), Tehran, Iran
e:mail: tayebrazi@yahoo.com

I. Bordi (✉)
Department of Physics, Sapienza University of Rome, Rome, Italy
e-mail: Isabella.bordi@roma1.infn.it

T. Raziei · L. S. Pereira
CEER-Biosystems Engineering, Institute of Agronomy, Technical University of Lisbon, Lisbon, Portugal

L. S. Pereira
e-mail: lspereira@isa.utl.pt

1 Introduction

Drought originates from a deficiency of precipitation (less than normal) over an extended period of time, and, as a natural phenomenon, can be considered an integrated part of climate variability. It may occur in all climatic zones and is triggered by large-scale features of the atmospheric circulation, such as high-pressure systems, winds carrying continental rather than oceanic air masses, or high temperatures. Such atmospheric conditions tend to reduce the amount of water vapor in the atmosphere that is the basic source for precipitation. However, drought characteristics vary significantly from one region to another due to local effects and its impact on local water resources availability compared to needs (Pereira et al. 2009). Thus, the identification of homogeneous regions within a country with distinct drought behaviours is of particular interest for drought risk assessment and for a more efficient water resources management at regional level.

Drought, however, cannot be viewed solely as a physical phenomenon but it must be considered in relation to its impacts on society. It is a creeping phenomenon that slowly sneaks up and impacts many sectors of the economy, the environment, and operates on many different time scales (Rossi 2000; Wilhite et al. 2007). For example, soil moisture responds to precipitation deficits occurring on a relatively short time scale, whereas groundwater, streamflow and reservoir storage respond to precipitation deficits arising over many months. The American Meteorological Society (1997) grouped drought definitions and types into four categories: meteorological, agricultural, hydrological and socioeconomic. Along the years, several indices have been developed to monitor these kinds of drought (Heim 2002; Keyantash and Dracup 2002). Particular interest has been devoted to the Standardized Precipitation Index (SPI, McKee et al. 1993), which for its characteristics (it is a standardized and multi-scale index; see next section) allows objectively comparing dry/wet conditions of regions with different hydrological regimes and evaluating the different kinds of drought.

Using the SPI and/or other indices, many authors have analyzed spatial modes and time variability of drought in different areas (see for example Soulé 1990; Bordi et al. 2001; Bonaccorso et al. 2003; Bordi and Sutera 2004; Bordi et al. 2006; Vicente-Serrano 2006; Raziei et al. 2009; Santos et al. 2010). However, spatial modes of drought over a region might change as a function of the time scale considered, i.e. the type of drought analyzed. Vicente-Serrano (2006) showed that using rain-gauge data over the Iberian Peninsula the spatial modes of droughts are conditioned to the SPI time scale, pointing out the increasing spatial complexity of drought modes as the time scale of the index is increased.

Precipitation, the basic variable for the SPI computation, is highly variable in Iran, both in space and in time. It is mainly controlled by the wide latitudinal extent (from 25 N to 40 N) and by the pronounced relieves (Zagros and Alborz mountain chains in the west and north, respectively). The moisture coming from the Mediterranean Sea and Persian Gulf is usually stopped by the Zagros Mountains. The lowland areas are open to the cold (dry) continental currents flowing from the northeast, and the mitigating influence of the Caspian Sea is limited to the northern regions of Alborz Mountains. There are regions in the south of the Caspian Sea and in the Zagros Mountains that receive up to 2000 mm of annual precipitation, whereas a portion of southern and eastern Iran gets less than 50 mm. Furthermore, most of precipitation falls during winter and autumn seasons due to the prevalence of humid westerly winds from the Mediterranean; differently, there are regions in northwest that have the largest share of precipitation during spring (see Raziei et al. 2008; 2010 and references therein). Due to the high variability of precipitation and frequent drought events, the increasing water demands for an ever growing population, for the agriculture and the

economic development, a rationale water management at country level is a difficult task in Iran, especially under drought conditions. Hence, the definition of sub-regions characterized by different drought variability is of great importance for water resources management and land use planning.

Recently, Raziei et al. (2011) have studied the spatio-temporal variability of hydrological drought over Iran using observational, gridded (Global Precipitation Climatology Centre, GPCC) and reanalysis (National Center for Environmental Prediction/National Center for Atmospheric Research, NCEP/NCAR) datasets. By applying the SPI on 12-month time scale, four sub-regions have been identified within the country. In another paper (Raziei et al. 2010), the authors showed similar results for the SPI on 3-, 6- and 24-month time scales, i.e. similar sub-regions were found using the same data (GPCC and NCEP/NCAR datasets with 2.5 and 1.9° resolution, respectively) and the same methodology (Principal Component Analysis and Varimax rotation). Thus, in depth investigations were suggested to better understand the sensitivity of the identified drought modes to the SPI time scale. The origin of the different sensitivity of drought regionalization in the Iberian Peninsula and Iran, in fact, might be due to the different precipitation regimes characterizing the two countries, or to the different spatial resolutions (or source) of data used for the analyses.

On these grounds, the present paper intends to investigate the sensitivity of regional drought modes in Iran with respect to the SPI time scales. Moreover, since the spatial resolution of the input data (precipitation in case of SPI), may have an impact on drought regionalization, also this aspect is addressed. A coarse spatial resolution, in fact, better represents the large-scale features of drought, while a finer resolution provides more information on local features and high-frequency fluctuations.

2 Data and Methods

The recent version of GPCC precipitation dataset covering the period 1951–2007 with 2.5, 1 and 0.5° resolution is used for the analysis. Drought conditions are assessed applying the SPI as defined by McKee et al. (1993). In representing the various kinds of drought, the time scales of 1-, 3-, 6-, 12-, 24- and 36-month are considered for the SPI computation. For a given spatial resolution and time scale, the S-mode Principal Component Analysis (PCA) and Varimax rotation are applied to the SPI field to search for aggregations of climate sub-regions that experienced similar drought (moisture) conditions during the study period.

2.1 Gridded Data

The GPCC Full Data Product Version 5, updated in December 2010, is a gauge-based gridded monthly precipitation dataset for the global land surface, available in 2.5, 1, 0.5 grid resolutions. The dataset covers the period 1901–2009 and is based on both non real-time and real-time stations (Schneider et al. 2010). GPCC monthly precipitation analysis products are based on anomalies from climatological normals at the stations, or from GPCC high-resolution gridded climatology where no station normal is available. The anomalies are spatially interpolated by the analysis method Spheremap (Willmott et al. 1985) and the gridded anomalies are then superimposed on the GPCC climatology 2010. The GPCC precipitation climatology (reference period 1951–2000) consists of normals collected by WMO, delivered by the countries to GPCC, or calculated from time series of monthly data (with at least 10 complete years of data) available in the GPCC data base (for details see the GPCC annual reports at http://gpcc.dwd.de). Recently, Raziei et al. (2010; 2011) have

assessed the spatial and temporal variability of drought over Iran using the GPCC Full Data Product Version 4 (previous version), finding good and satisfactory agreement with observations and NCEP/NCAR reanalysis, respectively.

For the present analysis only grid points over Iran are taken into account and the time section 1951–2007 is considered.

2.2 The SPI and PCA

Drought conditions are assessed through the SPI. The SPI computation for a given location and month of the year is based on the long-term precipitation record accumulated over the selected time scale. The empirical probability distribution of the accumulated precipitation is fitted to a theoretical distribution. Usually, the two-parameter Gamma distribution is used for fitting the observed precipitation distribution, even if in particular regions other choices may result more suitable (Guttman 1999). In the present study, the original definition of the SPI by McKee et al. (1993) is applied that is based on the two-parameter Gamma probability density function. The cumulative theoretical distribution is then transformed through an equal-probability transformation into a normal distribution. Thus, the SPI represents a Z-score, or the number of standard deviations above or below that a precipitation event is from the mean. Positive SPI values indicate greater than median precipitation, and negative values indicate less than median precipitation. For the purpose of the present paper the time scales of 1-, 3-, 6-, 12-, 24- and 36-month are considered in the SPI computation.

In identifying drought modes, for a given time scale, the S-mode PCA (Rencher 1998) is applied to the SPI field. The PCA consists in computing the covariance matrix of the SPI data with the corresponding eigenvalues and eigenvectors. The projection of the SPI fields onto the orthonormal eigenfunctions provides the principal components or PC score time series. The spatial patterns (eigenvectors), properly normalized (divided by their Euclidean norm and multiplied by the square root of the corresponding eigenvalues) are called "loadings" and represent the correlation between the original data (SPI time series at single grid points) and the corresponding principal component time series. More localized patterns are obtained by applying the Varimax rotation to selected loadings. Since such orthogonal rotation preserves the orthogonality in time, i.e. the rotated principal components are not correlated (Rencher 1998; Mestas-Nuñez 2000), the method allows finding sub-regions within the country that have rather independent drought behaviors. Following the rule by North et al. (1982), the sampling errors at 95 % confidence level of the eigenvalues associated with the principal components have been estimated, allowing to establish how many loadings to retain for rotation.

2.3 Congruence Coefficient

In assessing the degree of likeness between rotated loadings of the SPI on different time scales at a given GPCC spatial resolution, the vectors of the loadings matrices are compared using the congruence coefficient (Harman 1976):

$$g_{AB} = \frac{\sum_{j=1}^{n} \left(b_{jA} \times b_{jB}\right)}{\sqrt{\left(\sum_{j=1}^{n} b_{jA}^2\right) \times \left(\sum_{j=1}^{n} b_{jB}^2\right)}} \quad (1)$$

where b_{jA} is a loading from the rotated loading vector A from one solution, b_{jB} is a loading from the rotated loading vector B from another solution, and n is the number of

variables in each eigenvector, which for the S-mode PCA corresponds to spatial positions. The coefficient ranges in value from +1 for perfect agreement (or −1 for perfect inverse agreement) to 0 for no agreement. The congruence coefficient is preferred to the correlation coefficient for measuring pattern similarity because it preserves the mean (whereas the correlation coefficient measures deviations from the mean), and the mean is an important feature of a PC loading vector (Richman 1986; Guirguis and Avissar 2008). Following Richman (1986) and the references therein, the guidelines listed below are adopted as an indicator of the degree of likeness between patterns:

excellent≥0.98
0.98>good≥0.92
0.92>borderline≥0.82
0.82>poor≥0.68
terrible<0.68.

3 Results

In this section, regional drought modes based on the SPI computed on different time scales are illustrated for each spatial resolution of the GPCC dataset.

First, the PCA is applied to the SPI time series computed on the selected time scales (1-, 3-, 6-, 12-, 24- and 36-month) using the GPCC precipitation data with 2.5, 1, and 0.5° resolution. Secondly, based on the scree plot and the North's rule of thumb, for each SPI time scale and spatial resolution, the first loadings associated with the eigenvalues whose 95 % confidence intervals do not overlap have been retained for Varimax rotation. In Fig. 1 the scree plots for the different SPI time scales and GPCC spatial resolutions are shown. As can be noticed, for 2.5° resolution and SPI time scales 1–24 month the first four eigenmodes are independent and they are retained for Varimax rotation, while for 36-month time scale only the first two eigenmodes are selected. By considering the fine resolution of 1° and the time scales of 1-, 3- and 12-month the first four eigenmodes are retained for rotation, while for 6-month time scale the first three and for the longer time scales (24- and 36-month) only the first two eigenmodes. Lastly, for the higher resolution of 0.5°, the first four eigenmodes associated with 1-, 6- and 12-month time scales are considered for rotation, while the first three eigenmodes are taken into account for the remaining SPI time scales. The percentages of the total variance explained by the un-rotated and Varimax rotated PCs are listed in Table 1. It can be noted that the cumulative variance varies as a function of the SPI time scale and GPCC spatial resolution, but it is bounded between about 55 % and 75 %. A description of the rotated loadings (REOFs) obtained for each spatial resolution follows.

Let us consider first the GPCC dataset with 2.5° spatial resolution. The rotated loadings for the different SPI time scales are shown in Fig. 2. For the SPI on 1-month time scale (SPI-1, Fig. 2a), four sub-regions are identified (central-western, south-eastern, north-eastern and north-western), which are characterized by high positive loading values. Since by construction the rotated loading values represent the correlations between the SPI series and the corresponding rotated PC scores, a threshold value of 0.6–0.7 on the rotated loading is reasonable for spatially delimiting the sub-regions that experienced similar drought variability in the study period (orange and red areas in the maps). By increasing the time scale from 3- to 24-month, the four regional drought modes remain quite stable in their spatial homogeneity. On the longest time scale of 36-month, instead, only two sub-regions are

identified (Fig. 2f). In fact, due to the near degeneracy of the eigenvalues of the SPI covariance matrix (Fig. 1f), only two loadings have been retained for Varimax rotation. For time scales greater than 1-month, the accumulation procedure applied on monthly precipitation filters out high frequency fluctuations and only the long-term behaviours of the SPI time series emerge. This might enhance the correlation among the SPI series at

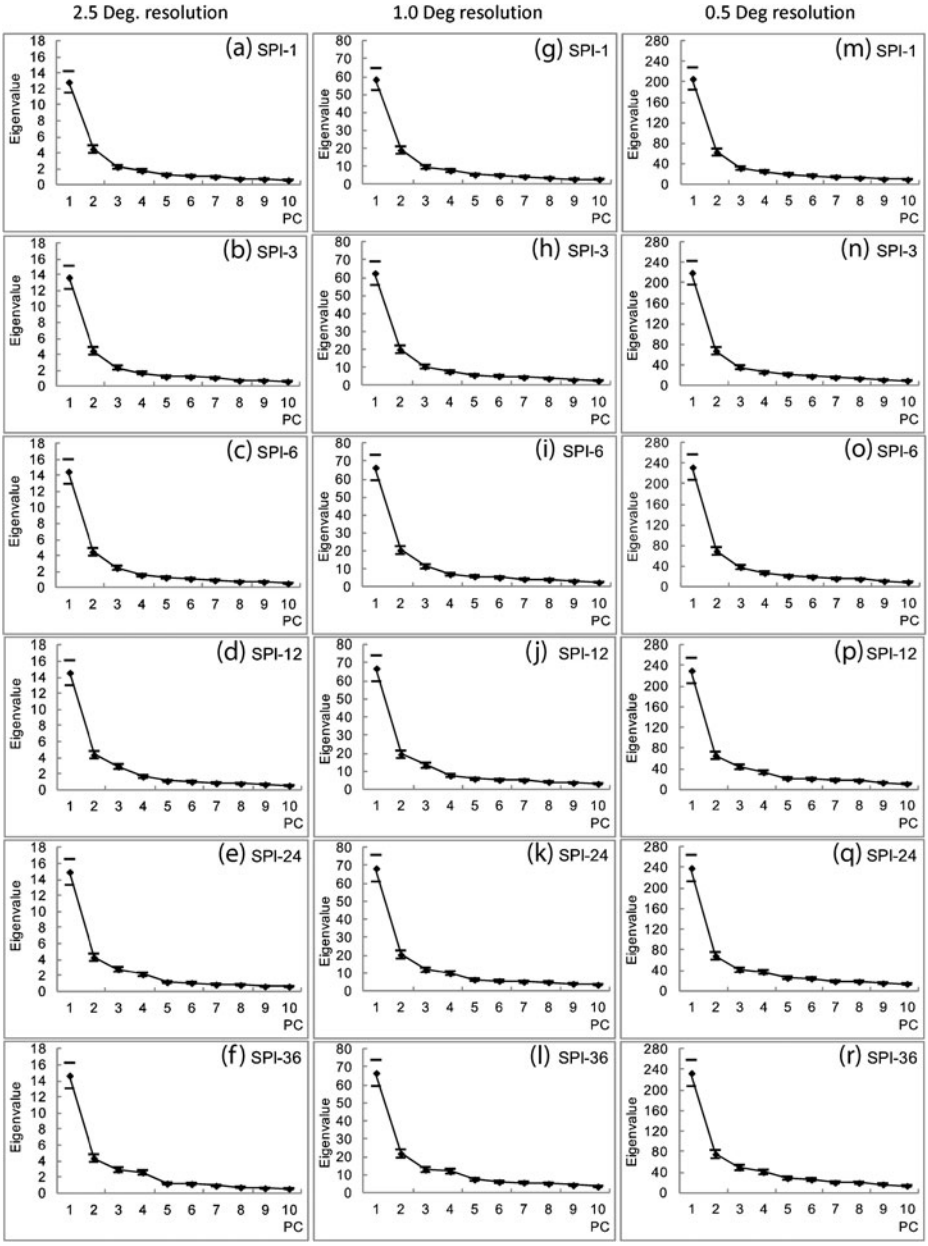

Fig. 1 First ten eigenvalues with the corresponding errorbars at 95 % confidence level resulting from the PCA applied to the SPI computed on different time scales and GPCC spatial resolutions

Table 1 Percentage of the total variance explained by the un-rotated (UR) and Varimax rotated (VR) loadings of the SPI on different time scales. Precipitation data are GPCC with 2.5, 1 and 0.5° resolution

GPCC 2.5° resolution	PC	SPI-1		SPI-3		SPI-6		SPI-12		SPI-24		SPI-36	
		UR	VR	UR	VR	UR	VR	UR	VR	UR	VR	UR	VR
	1	40.3	18.6	42.8	20.8	45.3	24.6	45.5	24.7	46.7	25.6	45.8	31.1
	2	14.0	17.9	13.9	18.6	13.9	19.9	13.7	23.2	13.4	24.9	13.6	28.3
	3	7.0	16.6	7.3	15.4	7.7	13.7	9.1	16.3	8.6	14.7	-	-
	4	5.5	13.6	5.2	14.4	4.8	13.5	5.2	9.2	6.7	10.1	-	-
	Total	66.7	66.7	69.2	69.2	71.7	71.7	73.4	73.4	75.3	75.3	59.5	59.5
GPCC 1° resolution	PC	SPI-1		SPI-3		SPI-6		SPI-12		SPI-24		SPI-36	
		UR	VR	UR	VR	UR	VR	UR	VR	UR	VR	UR	VR
	1	34.1	17.6	36.3	18.9	38.6	22.8	39.0	22.1	39.8	26.1	38.8	26.6
	2	11.1	14.3	11.7	15.0	11.9	17.8	11.3	20.3	11.9	25.6	12.7	24.9
	3	5.6	12.9	6.1	13.5	6.6	16.6	7.8	13.1	-	-	-	-
	4	4.5	10.5	4.4	11.1	-	-	4.5	7.0	-	-	-	-
	Total	55.3	55.3	58.5	58.5	57.2	57.2	62.6	62.6	51.7	51.7	51.5	51.5
GPCC 0.5° resolution	PC	SPI-1		SPI-3		SPI-6		SPI-12		SPI-24		SPI-36	
		UR	VR	UR	VR	UR	VR	UR	VR	UR	VR	UR	VR
	1	32.8	16.8	34.9	19.7	36.9	22.0	36.6	21.8	37.9	22.6	37.0	23.2
	2	10.0	13.1	10.7	15.8	11.0	15.6	10.5	18.4	10.9	21.3	11.9	20.8
	3	5.0	11.5	5.6	15.7	6.1	11.0	7.0	10.5	6.5	11.4	7.8	12.7
	4	4.0	10.3	-	-	4.3	9.7	5.3	8.6	-	-	-	-
	Total	51.7	51.7	51.2	51.2	58.3	58.3	59.3	59.3	55.3	55.3	56.7	56.7

different grid points, providing an explanation of the reduced number of drought modes found for time scales longer than 1-month. Following this reasoning, since the spatial resolution of 2.5° already captures the large-scale features of drought, only very long time scales, like 36-month, show this effect due to degenerate eigenvalues. For finer spatial resolutions, instead, such an effect might occur also for short time scales. It is worth noting that the results obtained are in close agreement with those found by Raziei et al. (2010) using the GPCC Full Data Product Version 4 for the period 1948–2007 and applying the same methodology.

Now let us consider the GPCC dataset with 1° spatial resolution. The rotated loadings are shown in Fig. 3. Four regional drought modes are found for the SPI on 1-, 3, 12-month time scale, three modes for 6-month and two modes for the longer time scales of 24- and 36-month. The most stable drought mode (i.e. identified for all time scales) represents the southeast region of Iran, but its area extension and spatial inhomogeneity seems to increase as the SPI time scale increases. It explains a percentage of the total variance ranging from about 14 % to about 25 % depending on the time scale considered. The remaining three regional modes identified for 1-, 3- and 12-month time scales appear merged into two or one mode when different time scales are considered (Fig. 3c, e, f).

Lastly, results for GPCC with 0.5° resolution are shown in Fig. 4. Four drought modes are identified for 1-, 6- and 12-month time scale (Fig. 4a, c, d), while for the other time scales the modes are reduced to three (Fig. 4b, e, f). As discussed by Vicente-Serrano (2006), the degree of spatial complexity of drought modes seems to increase as the time scale of the index is increased. Certainly, the reduced number of modes for 24- and 36-month time scales enhances this feature. However, comparing the results obtained so far for the three spatial

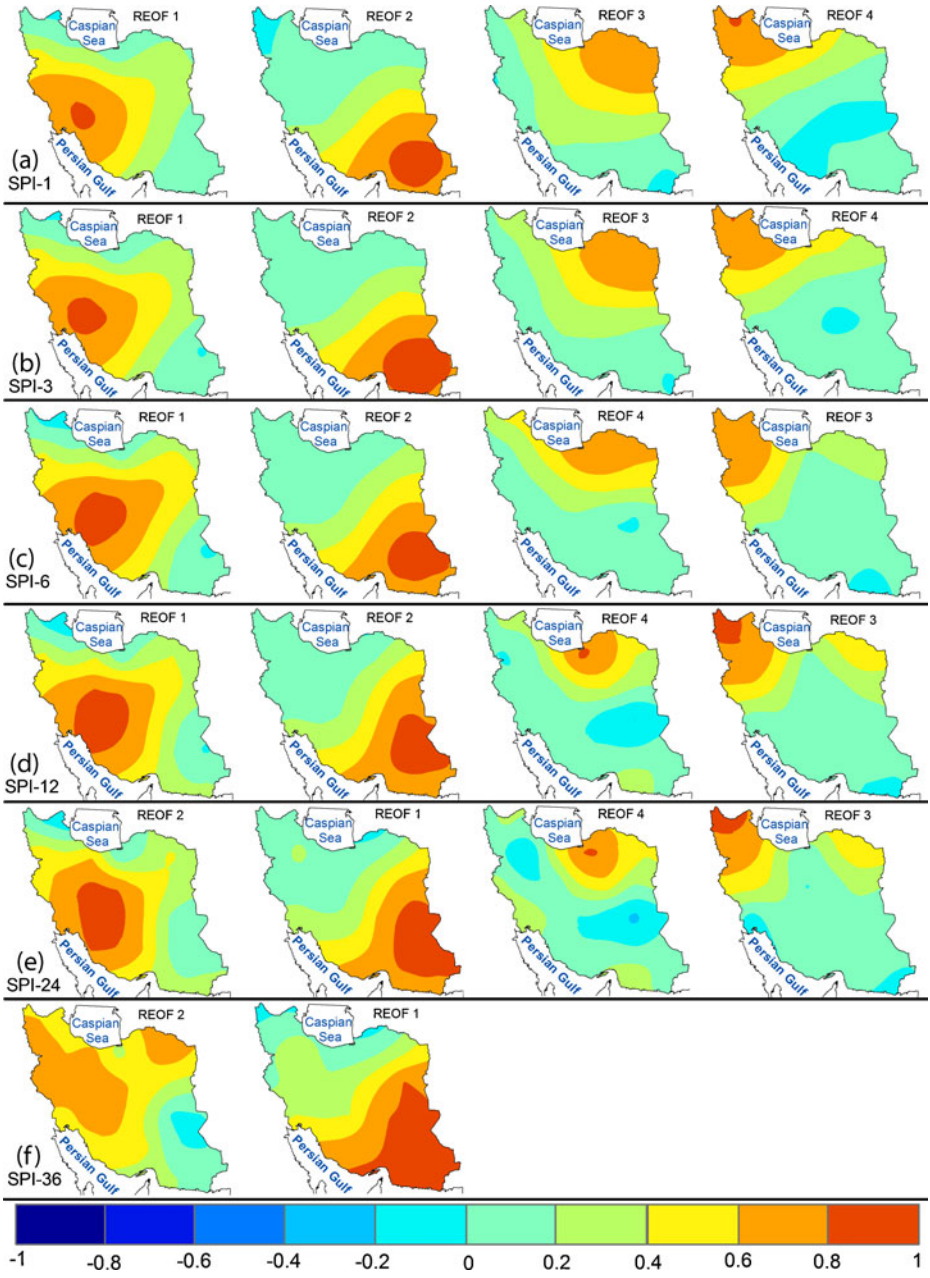

Fig. 2 Varimax rotated loadings (REOFs) of the SPI on different time scales computed using GPCC precipitation data with 2.5° resolution. Sub-regions are identified by loading values greater than 0.6–0.7 (orange and red areas)

resolutions, it appears that the dependence of the regional modes on the SPI time scale is greater when a finer resolution is considered. Moreover, it emerges that for the same number of drought modes those obtained with the finer resolution explain less percentage of the total

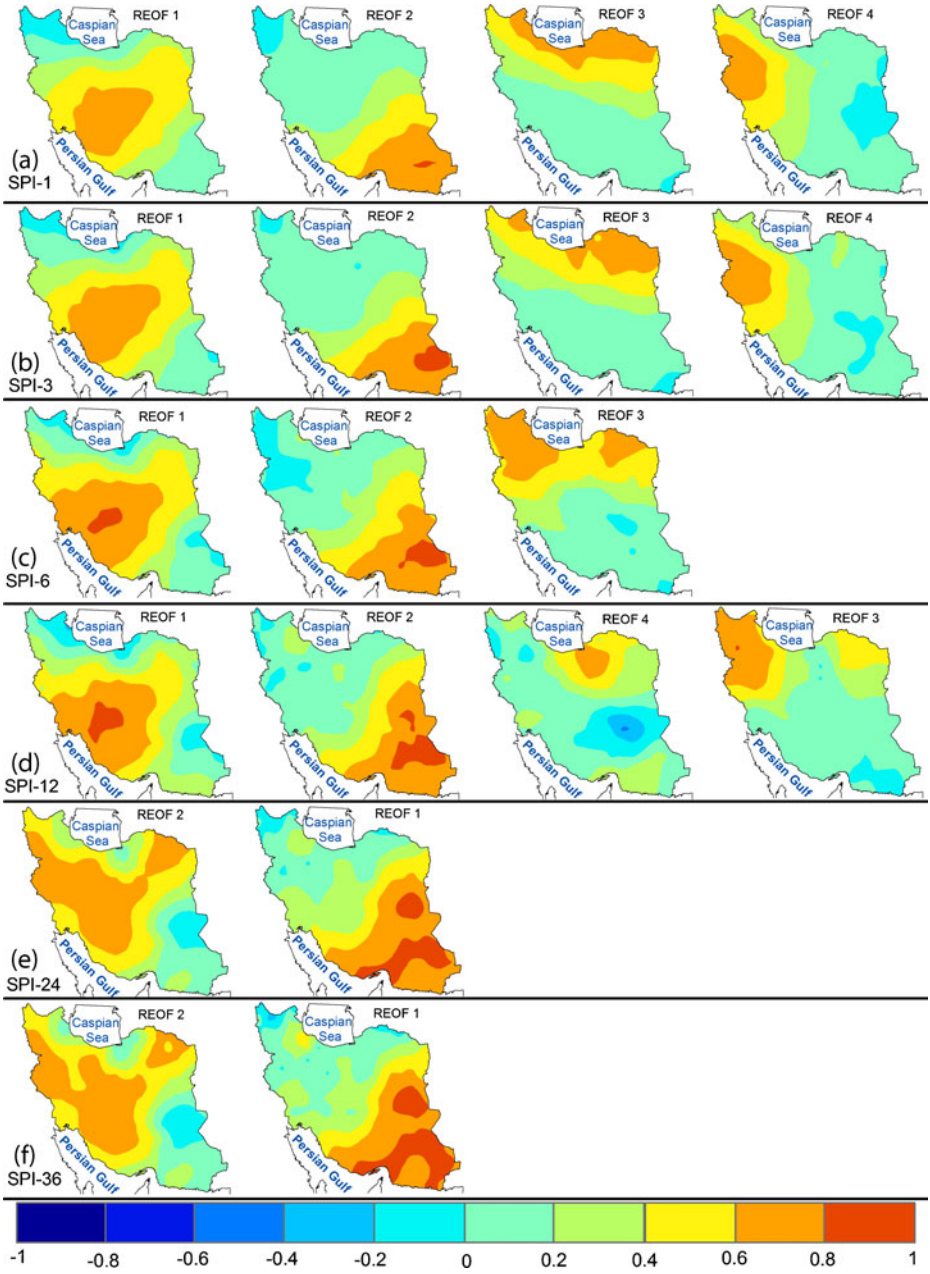

Fig. 3 As in Fig. 2 but for GPCC precipitation data with 1° resolution

variance compared with the ones for the coarse resolution. Results are consistent with the greater spatial variability captured by the finer resolution that the PCA tries to maximize and the Varimax rotation to group into a few areas of common variability.

For a given spatial resolution, the degree of similarity between rotated PC solutions at different time scales is assessed by quantitatively comparing their respective loading

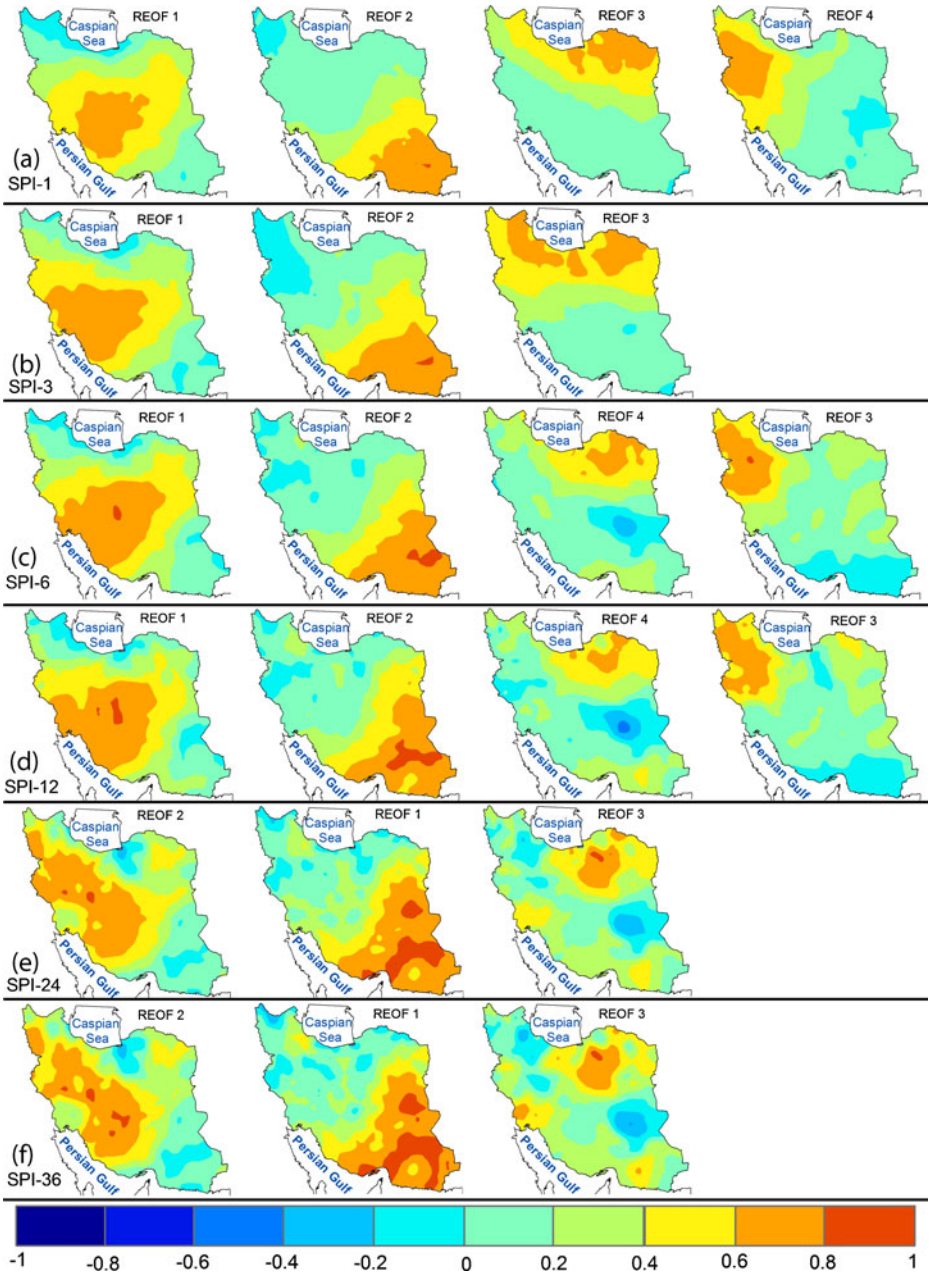

Fig. 4 As in Fig. 2 but for GPCC precipitation data with 0.5° resolution

matrices computing the congruence coefficients (Harman 1976; White et al. 1991). As an example, the congruence coefficients for the rotated loadings at 2.5° resolution (Fig. 2) are listed in Table 2. It should be noting that the REOF-2 of the SPI on 36-month time scale is used to compute the congruence coefficients for the north-eastern and north-western sub-regions. Results are consistent with the conclusions discussed so far based on a visual comparison of the

Table 2 Congruence coefficients for the rotated loadings shown in Fig. 2 (2.5° resolution). To better highlight the differences among the coefficients they are listed in three decimal places

Central-western sub-region	SPI-3 REOF-1	SPI-6 REOF-1	SPI-12 REOF-1	SPI-24 REOF-2	SPI-36 REOF-2
SPI-1 REOF-1	0.996	0.982	0.981	0.971	0.859
SPI-3 REOF-1	1	0.991	0.985	0.972	0.851
SPI-6 REOF-1		1	0.993	0.974	0.851
SPI-12 REOF-1			1	0.989	0.855
SPI-24 REOF-2				1	0.886
South-eastern sub-region	SPI-3 REOF-2	SPI-6 REOF-2	SPI-12 REOF-2	SPI-24 REOF-1	SPI-36 REOF-1
SPI-1 REOF-2	0.998	0.990	0.964	0.961	0.956
SPI-3 REOF-2	1	0.991	0.964	0.961	0.955
SPI-6 REOF-2		1	0.990	0.986	0.972
SPI-12 REOF-2			1	0.998	0.981
SPI-24 REOF-1				1	0.988
North-eastern sub-region	SPI-3 REOF-3	SPI-6 REOF-4	SPI-12 REOF-4	SPI-24 REOF-4	SPI-36 REOF-2
SPI-1 REOF-3	0.996	0.931	0.798	0.767	0.758
SPI-3 REOF-3	1	0.949	0.827	0.798	0.763
SPI-6 REOF-4		1	0.942	0.881	0.774
SPI-12 REOF-4			1	0.961	0.659
SPI-24 REOF-4				1	0.644
North-western sub-region	SPI-3 REOF-4	SPI-6 REOF-3	SPI-12 REOF-3	SPI-24 REOF-3	SPI-36 REOF-2
SPI-1 REOF-4	0.995	0.953	0.939	0.905	0.757
SPI-3 REOF-4	1	0.971	0.962	0.928	0.800
SPI-6 REOF-3		1	0.985	0.958	0.809
SPI-12 REOF-3			1	0.985	0.822
SPI-24 REOF-3				1	0.795

rotated loadings. It is found that the congruence coefficients between the REOFs in Fig. 2 associated with the central-western sub-region are greater than 0.97 (excellent/good spatial congruence) for time scales from 1 to 24 months, while those between the same REOFs and the one for 36-month time scale range between 0.85 and 0.88 (borderline congruence). To be noted is the excellent/good spatial congruence among the rotated loadings associated with the south-eastern sub-region (congruence coefficients greater than 0.96). For the north-eastern sub-region, instead, good congruence is found between the rotated loadings associated with short SPI time scales, while poor spatial congruence emerges for the patterns related to long time scales. Lastly, for the north-western sub-region good spatial congruence is found among the REOFs of the SPI from 1 to 24-month time scale, while there is poor congruence between them and the REOF-2 of the SPI on 36-month time scale. Thus, as expected, the low values of the congruence coefficients are due to the reduced number of loadings retained for Varimax rotation at 36-month time scale that did not allow to clearly define the four sub-regions, with the exception of the south-eastern one. Similar results are found for the other GPCC spatial resolutions (here not shown to limit the length of the paper), i.e. excellent/good congruences among REOFs at all the considered time scales are found only for the south-eastern sub-region.

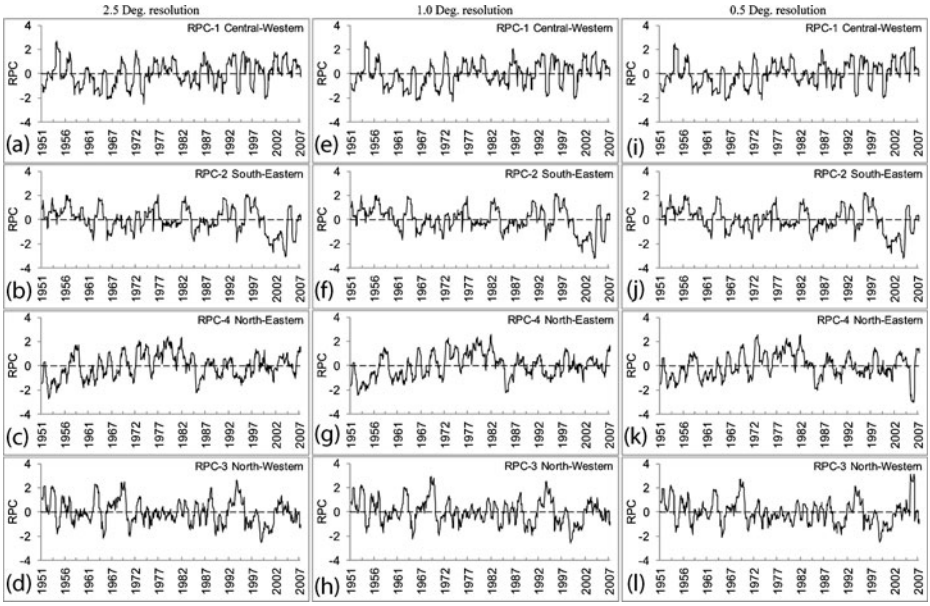

Fig. 5 Rotated principal component score time series (RPCs) obtained for the SPI on 12-month time scale at different GPCC spatial resolutions and associated with the rotated loadings shown in Figs. 2, 3 and 4

Finally, to give an idea of the time behaviours of drought in the identified sub-regions, the rotated principal component score time series (RPCs) for the 12-month time scale and different spatial resolutions are shown in Fig. 5. For a given spatial resolution of GPCC data, the figure, as expected, reveals different time behaviours in the four identified sub-regions. By increasing the spatial resolution from 2.5 to 0.5°, the RPCs associated with the same sub-regions show a good agreement; some discrepancies are noticeable only for the north-eastern and north-western sub-regions that explain the lower percentages of variance and are the less well-defined regions.

4 Conclusions

In the present paper, the sensitivity of regional drought modes in Iran to the SPI time scale and to the different spatial resolution of precipitation data is investigated. The analysis is performed using the GPCC datasets with 2.5, 1, and 0.5° resolution covering the period 1951–2007. The SPI on 1-, 3-, 6-, 12-, 24- and 36-month time scales is computed according to the original definition by McKee et al. (1993). The S-mode PCA and Varimax rotation are applied to the SPI fields to search for aggregations of climate regions that experienced similar drought variability during the study period. Results suggest that the spatial resolution of precipitation data influences the sensitivity of the identified drought modes to the SPI time scale. In particular, when finer spatial resolutions (compared to 2.5°) of precipitation data are considered, the number and homogeneity of drought modes varies as the time scale is increased from 1- to 36-month. Moreover, the south-eastern sub-region is found to be the most stable (i.e. identified in all cases here addressed), while the others are more vulnerable to variations in the SPI time scale and data resolution.

Further applications in other regions are suggested to verify the role played by the spatial resolution of the input data on drought regionalization when different SPI time scales are considered.

Acknowledgements GPCC gridded precipitation data (Full Data Product Version 5) were freely provided by the Deutscher Wetterdienst through their web site http://www.dwd.de.

References

American Meteorological Society (AMS) (1997) Meteorological drought-policy statement. Bull Amer Meteorol Soc 78:847–849

Bonaccorso B, Bordi I, Cancelliere A, Rossi G, Sutera A (2003) Spatial variability of drought: An analysis of the SPI in Sicily. Water Resour Manage 17:273–296

Bordi I, Frigio S, Parenti P, Speranza A, Sutera A (2001) The analysis of the standardized precipitation index in the Mediterranean area: Large-scale patterns. Ann Geofis 44:965–978

Bordi I, Sutera A (2004) Drought variability and its climatic implications. Glob Planet Change 40:115–127

Bordi I, Fraedrich K, Petitta M, Sutera A (2006) Large-scale assessment of drought variability based on NCEP/NCAR and ERA-40 re-analyses. Water Resour Manage 20:899–915

Guirguis KJ, Avissar R (2008) A precipitation climatology and dataset intercomparison for the western United States. J Hydrometeor 9:825–841

Guttman NB (1999) Accepting the standardized precipitation index: A calculation algorithm. J Amer Water Resour Ass 35:311–322

Harman HH (1976) Modern factor analysis. 3rd ed. The University of Chicago Press, pp 487

Heim RR Jr (2002) A review of twentieth-century drought indices used in the United States. Bull Amer Meteorol Soc 83:1149–1165

Keyantash J, Dracup JA (2002) The quantification of drought: An evaluation of drought indices. Bull Amer Meteorol Soc 83:1167–1180

McKee TB, Doesken NJ, Kleist J (1993) The relationship of drought frequency and duration to time scales, *In Proceeding of the 8th Conference on Applied Climatology*, 17–22 January, Anaheim, CA. Amer Meteorol Soc, Boston, pp 179–184

Mestas-Nuñez AM (2000) Orthogonality properties of rotated empirical modes. Int J Climatol 20:1509–1516

North GR, Bell TL, Cahalan RF (1982) Sampling errors in the estimation of empirical orthogonal functions. Mon Wea Rev 110:699–706

Pereira LS, Cordery I, Iacovides I (2009) Coping with water scarcity: Addressing the challenges. Springer, Dordrecht, 382 p

Raziei T, Bordi I, Pereira LS (2008) A precipitation-based regionalization for western Iran and regional drought variability. Hydrol Earth Syst Sci 12:1309–1321

Raziei T, Saghafian B, Paulo AA, Pereira LS, Bordi I (2009) Spatial and temporal variability of drought in western Iran. Water Resour Manage 23:439–455

Raziei T, Bordi I, Pereira LS, Sutera A (2010) Space-time variability of hydrological drought and wetness in Iran using NCEP/NCAR and GPCC datasets. Hydrol Earth Syst Sci 14:1919–1930

Raziei T, Bordi I, Pereira LS (2011) An application of GPCC and NCEP/NCAR datasets for drought variability analysis in Iran. Water Resour Manage 25:1075–1086

Rencher AC (1998) Multivariate statistical inference and applications. John Wiley & Sons, Inc

Richman MB (1986) Rotation of principal components. Int J Climatol 6:293–335

Rossi G (2000) Drought mitigation measures: a comprehensive framework. In: Vogt JV, Somma F (eds) Drought and drought mitigation in Europe. Kluver Academic Publishers, Dordrecht, pp 233–246

Santos JF, Pulido-Calvo I, Portela MM (2010) Spatial and temporal variability of droughts in Portugal. Water Resour Res 46:W03503. doi:10.1029/2009WR008071

Schneider U, Becker A, Meyer-Christoffer A, Ziese M, Rudolf B (2010) Global precipitation analysis products of the GPCC. Global precipitation climatology centre (GPCC), DWD, internet publication (http://www.dwd.de)

Soulé PT (1990) Spatial patterns of multiple drought types in the contiguous United States: A seasonal comparison. Clim Res 1:13–21

Vicente-Serrano SM (2006) Differences in spatial patterns of drought on different time scales: An analysis of the Iberian Peninsula. Water Resour Manage 20:37–60

White D, Richman M, Yarnal B (1991) Climate regionalization and rotation of principal components. Int J Climatol 11:1–25

Wilhite DA, Svoboda MD, Hayes MJ (2007) Understanding the complex impacts of drought: A key to enhancing drought mitigation and preparedness. Water Resour Manage 21:763–774

Willmott CJ, Rowe CM, Philpot WD (1985) Small-scale climate maps: A sensitivity analysis of some common assumptions associated with grid-point interpolation and contouring. Amer Cartographer 12:5–16